



UNIVERSITY OF LEEDS

This is a repository copy of *Disturbance Rejection in Multi-DOF Local Magnetic Actuation for Robotic Abdominal Surgery*.

White Rose Research Online URL for this paper:
<http://eprints.whiterose.ac.uk/126708/>

Version: Accepted Version

Article:

Leong, F, Mohammadi, A, Tan, Y et al. (4 more authors) (2018) Disturbance Rejection in Multi-DOF Local Magnetic Actuation for Robotic Abdominal Surgery. *IEEE Robotics and Automation Letters*, 3 (3). pp. 1568-1575. ISSN 2377-3766

<https://doi.org/10.1109/LRA.2018.2800795>

© 2018 IEEE. Personal use of this material is permitted. Permission from IEEE must be obtained for all other uses, in any current or future media, including reprinting/republishing this material for advertising or promotional purposes, creating new collective works, for resale or redistribution to servers or lists, or reuse of any copyrighted component of this work in other works.

Reuse

Items deposited in White Rose Research Online are protected by copyright, with all rights reserved unless indicated otherwise. They may be downloaded and/or printed for private study, or other acts as permitted by national copyright laws. The publisher or other rights holders may allow further reproduction and re-use of the full text version. This is indicated by the licence information on the White Rose Research Online record for the item.

Takedown

If you consider content in White Rose Research Online to be in breach of UK law, please notify us by emailing eprints@whiterose.ac.uk including the URL of the record and the reason for the withdrawal request.



eprints@whiterose.ac.uk
<https://eprints.whiterose.ac.uk/>

Disturbance Rejection in Multi-DOF Local Magnetic Actuation for Robotic Abdominal Surgery

F. Leong¹, A. Mohammadi¹, Y. Tan¹, D. Thiruchelvam², C. Y. Lai³, P. Valdastrì⁴ and D. Oetomo²

Abstract—The potential of multi-degrees-of-freedom (DOFs) local magnetic actuation (LMA) has been established in recent years for dexterous minimally invasive surgical manipulations. Nonetheless, having multiple magnetic based units, one for each DOF, within a close vicinity to each other leads to magnetic field interaction among the magnetic sources, hence resulting in a disturbance to a given LMA unit. It is further realised that the disturbance is a result of actuation effort by the neighbouring magnetic sources forming the LMA units, and that the actuation command to all LMA units is a known information to the controller. Therefore, partial information of the disturbance is known and can be exploited in a disturbance rejection strategy. In this paper, this disturbance is modelled and used to augment a simplified model of the systems dynamics of the LMA-based surgical manipulators. The internal model principle (IMP) strategy is selected in which an observer is designed to estimate the disturbance to be rejected. Numerical simulation as well as experimental validation were performed to validate the efficacy of the IMP. The results serve to remove a significant technical hurdle in bringing the new emerging technique of Local Magnetic Actuation into practical reality for abdominal surgeries.

Index Terms—Medical Robots and Systems, Surgical Robotics: Laparoscopy, Abdominal Surgery, Magnetic Actuation.

I. INTRODUCTION

IN recent years, the use of magnetic devices has gained popularity across minimally invasive surgical (MIS) procedures for the abdominal cavity with the state-of-the-art reviewed in [1]. Concepts such as magnetic couplings have been utilised to anchor surgical devices onto the inside of the abdominal wall to the external magnets in abdominal surgeries. The key advantage of this approach is the removal of the rigid mechanical links from the outside into the abdominal cavity to support or manoeuvre surgical tools, which when used appropriately, has the potential of providing surgeons with more flexibility for the surgical manipulation.

Manuscript created September 10, 2017; revised December 21, 2017. The research reported in this article was supported in part by the Royal Society under grant number CH160052 and by the Engineering and Physical Sciences Research Council (EPSRC) under grant number EP/P027938/1. Any opinions, findings and conclusions, or recommendations expressed in this article are those of the authors and do not necessarily reflect the views of the Royal Society or the EPSRC.

¹ Florence Leong, Alireza Mohammadi, Ying Tan and Denny Oetomo are with the Melbourne School of Engineering, The University of Melbourne, Australia. {florence.leong,alirezam,yingt,doetomo}@unimelb.edu.au

² Dhan Thiruchelvam is with the Department of Surgery, University of Melbourne at St Vincent's Hospital

³ Chow Yin Lai is with the Royal Melbourne Institute of Technology (RMIT). chowyin.lai@rmit.edu.au

⁴ Pietro Valdastrì is with the School of Electronic and Electrical Engineering, University of Leeds, UK. p.valdastrì@leeds.ac.uk

Digital Object Identifier (DOI): see top of this page.

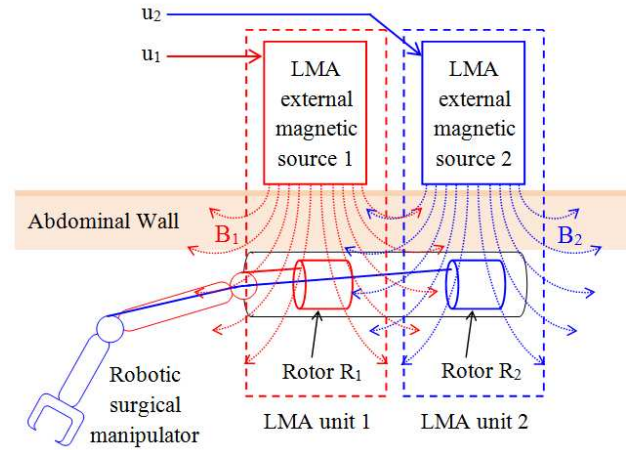


Fig. 1. An LMA system actuating a robotic surgical manipulation [29]. Two rotors on the inside of the abdominal wall are actuated by externally located stator 1 and 2, respectively. u_1 and u_2 are the actuating commands to regulate the motions of rotors R_1 and R_2 , respectively, through magnetic fields B_1 and B_2 . Disturbance happens when B_1 also affects rotor 2 and B_2 affects rotor 1.

Magnets have been successfully used to guide surgical devices to desired positions around the abdominal cavity through manual manipulation, such as in the Magnetic Anchoring and Guidance Systems (MAGS) [2], [3]. It has also been successfully utilised to directly manipulate objects within the body, such as shown in Octomag [4], [5], [6], [7], or to operate robotic manipulators mounted on a MAGS platform. The latter category allows a robotic manipulator to be mounted on a platform anchored to the inside of the abdominal wall, where the robotic manipulator can be motion-controlled, thus further improving and extending the mobility and dexterity available to the surgeons. Such manipulators can be realised through DC motors [8], [9]. Nonetheless, the miniaturised DC motors are limited in mechanical power due to the size limitation involved in this application [see Table III in [10]], thus is not scalable to generate sufficient force and speed required for various surgical tasks (see Table I).

Local Magnetic Actuation (LMA) [16] removes the need for a rigid link transmission to the internal surgical device (thus increasing mobility of the device within the abdominal cavity) while allowing the scalable actuation components to remain external, thus less affected by the size constraint. It utilises an external source of magnetic field to rotate an internal rotor located immediately on the other side of the abdominal wall, which is used to actuate the robotic manipulator inside of the abdominal cavity (see Figure 1). Multiple rotors (thus multiple

TABLE I
APPROXIMATE FORCE AND SPEED REQUIRED IN VARIOUS SURGICAL TASKS

Surgical tasks	Force	Speed	Ref
Liver and gall bladder retraction	6.6 N	N/A	[11]
Surgical camera	0.2 N	18 deg/s	[1]
Surgical manipulation (e.g. pushing)	5 N	<360 deg/s	[1]
Soft tissue (e.g. liver penetration)	0.08 N	1 mm/s	[12]
Soft tissue (e.g. liver resection)	0.9 N	3 mm/s	[13]
Suturing (on soft tissue, e.g. skin)	1.7 N	5 mm/s	[14]
Suturing (pulling and tying knot)	8 N	N/A	[15]

degrees of freedom (DOFs)) systems have been demonstrated to be feasible for surgical manipulation capability inside the abdominal cavity through an *in vivo* animal setting [17].

A realistic surgical robotic task would require multi-DOF manipulation. Each degree of actuation in the LMA concept involves the use of one powered external platform that generates a rotating magnetic field that interacts with an internal permanent magnet rotor. This means multiple sets (N sets) of the LMA units are required to realise an N -DOF surgical robot within the abdominal cavity.

It should be noted that there is only a limited amount of abdominal wall surface for the N sets of LMA units to be mounted. Thus the LMA units need to be arranged close to each other. The proximity to other LMA units mean that the magnetic field generated by a nearby LMA unit will interfere with the magnetic field actuating the rotor of a given LMA unit, resulting in a disturbance to the performance of the given LMA unit [18] (See Figure 1). Hence, to achieve a motion control performance of the surgical robotic manipulator within the available space constraint in the face of the disturbances, an effective means of disturbance rejection is required.

In this setting, the magnetic field disturbance on a given rotor is a result of the actuation command to the neighbouring rotors, which is a known information to the controller. How it propagates, attenuates and finally interacts with neighbouring rotors is however dependent on the external factors. In this case, partial information about the disturbance, such as the frequency of the disturbance signal, is available and thus exploited in this paper through the use of Internal Model Principle (IMP) to construct an effective disturbance rejection strategy [20], [21].

In the author's previous work, linear controllers such as the standard Proportional Integral (PI) implemented through a Field Oriented Control (FOC) was investigated [10], [22] for a single LMA unit. This work is extended in this paper to consider the case of multiple LMA units in simultaneous operation, thus introducing the systematic disturbance caused by the actuating signals of the neighbouring magnetic sources in this magnetic based surgical robotic system. This disturbance is demonstrated in this paper to be significant, even when a PI controller is in place. The partial information elaborated above is therefore exploited to incorporate an IMP based controller with the original PI controllers. The IMP based controller estimates the state of disturbance model and rejects

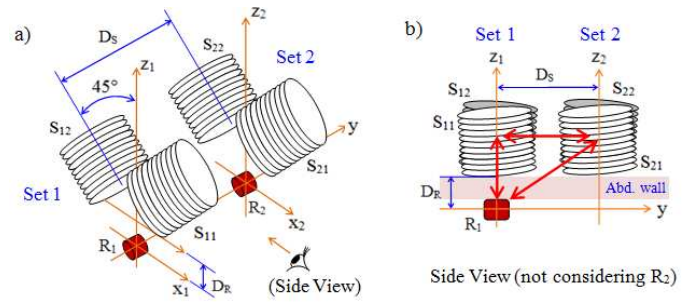


Fig. 2. A schematic diagram of the two-DOF LEMA system, a) 3D illustration and b) side view of the system with the magnetic interactions (depicted by the red arrows) among the stator sets and the rotor, R_1 , with a neighbouring rotor, R_2 being negligible.

the disturbances. The approach is implemented numerically and validated experimentally on an LMA system with two (neighbouring) LMA units, without any loss of generality in the applicability of the outcomes.

The remainder of the paper is organised as follows. Section II describes the model of LMA implementing the FOC strategy and the construction of the disturbance model. This disturbance model is then augmented with the model of the system for the implementation of IMP and the design by using observer for disturbance rejection in Section III. The simulation as well as the experimental setup and methodology are described in Section IV. The results and validation of IMP are presented and discussed in Section V.

II. MATHEMATICAL MODEL OF LEMA SYSTEM

Electromagnets, as opposed to rotating permanent magnets [16], are utilised in this paper for their ease in generating the arbitrary actuation magnetic field required by the control law. To denote the electromagnet version of LMA, the term LEMA (Local ElectroMagnetic Actuation) is used in this paper. The schematic diagram of the two-DOF LEMA configuration is shown in Figure 2. It illustrates two sets of LEMA systems (i.e. stators-rotor sets) that are placed in a close vicinity with a distance of D_s . Each stator sets consist of two (external) stators which drive one internal rotors that is located at a distance D_R away, simulating the average thickness of the abdominal wall. When a stator set is actuated to drive its corresponding rotor, the resulting magnetic field also affect rotors from the neighbouring set(s) of LEMA units. This magnetic interference generates disturbances onto the rotors, affecting their angular velocity. The disturbances can be treated as input disturbances. It is well-known that if some information of the input disturbances is available, it is possible to use internal model principle (IMP) based control design method to eliminate the effect of the input disturbances, which is investigated in this paper.

In this study, the model of the multi-DOF LEMA system presented in [18] is utilized. For the LEMA system i , its rotors are labeled as R_i . Each R_i is actuated by two stator coils, denoted as S_{ij} , where $j = \{1, 2\}$, respectively.

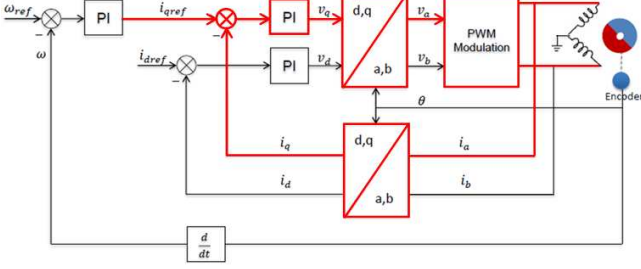


Fig. 3. Block diagram of the FOC method implemented through PI controllers for currents (inner loop) and angular velocity (outer loop) controls of the rotor R_i [22]. The inner loop that regulates current i_q connected to the outer loop is depicted in red.

A. Modelling of LEMA with FOC

Field-Oriented Control (FOC) has been widely implemented in permanent magnet synchronous motors (PMSMs) [23], [24]. The effectiveness of FOC has been demonstrated on the LEMA system [10], [22]. Another technique, the Sensorless Scalar Control (SSC), which is an open-loop strategy, has also been investigated in the past. A direct comparison between SSC and FOC for the LEMA application had found FOC to be superior in providing maximum transmittable torque, resulting in better steady-state performance and lower possibility of stall with the presence of closed-loop feedback [10].

The basic concept of FOC is to transform the sinusoidal currents of each stator in the system into a direct (d) - quadrature (q) frame which rotates together with the magnetic flux on the permanent magnet rotor. This transformation is useful as it is challenging for controllers to track time-varying sinusoidal signals in high speed [25]. In the d-q coordinate, the sinusoidal stator currents are converted to constant currents and can be controlled directly without any dependency on the rotor position. The control signals are then converted back to the original frame to drive the stators. The block diagram of the FOC implemented with a PI controller is as shown in Figure 3.

The FOC is implemented with an outer loop and an inner loop. The outer loop regulates the angular velocity while the inner loops regulate the currents i_q and i_d of the stators in the d-q frame, and provides the reference to the inner loop regulating i_q . The inner loop regulating i_d has a reference of zero, hence is independent of the outer loop. The control objective of the LEMA system is therefore to drive the output angular velocity to the reference (ω_{ref}). In order to simplify the analysis and design for disturbance rejection, the following assumption is made.

Assumption 1: By tuning parameters of PI controllers in the inner loop and outer loop appropriately, the inner loop in each LEMA units responds much faster than its outer loop such that the inner loop is stable. ◦

Remark 1: By using Singular Perturbation technique [26], the stability of the overall LEMA system, which consists of an inner loop, an outer loop and the controller, will be obtained by using the stability properties of the simplified system, in which the inner loop is ignored. In other words, the inner loop dynamics can be treated as a constant. Hence the controller

is designed for the simplified system to ensure the stability of the overall system, as stated in Remarks 2 and 3. ◦

With the settings explained above, as Assumption 1 holds, a simplified system of the i^{th} LEMA system is thus obtained. This simplified system ignores the dynamics of the faster inner loop, leading to a simpler model that can be used for IMP design in the next Section. The simplified system can be represented as a first-order system, applicable to each rotor R_i :

$$\dot{\omega} = -\frac{b}{J}\omega + \frac{\Psi_R}{J}i_{qref}, \quad (1)$$

where J and b denote the total moment of inertia and the friction coefficient of the rotor R_i respectively, Ψ_R is the magnetic flux at rotor R_i , i_{qref} is the reference i_q current to the inner loop and ω is the angular velocity of rotor R_i .

This model is a linear-time-invariant system (A, B, C) and can be represented in the state space form:

$$\begin{aligned} \dot{x} &= Ax + Bu \\ y &= Cx \end{aligned} \quad (2)$$

where state $x = \omega$ and the system input, $u = i_{qref}$, and with the following matrices:

$$A = -\frac{b}{J}, \quad B = \frac{\Psi_R}{J}, \quad C = 1. \quad (3)$$

In order to track the set-point, an integral action is incorporated, by introducing a new state x_{int} , which is an integral of the tracking error:

$$x_{int}(t) = \int_0^t e(\tau) d\tau, \quad (4)$$

where $e = r - y$. Here r is the reference velocity, ω_{ref} and C is defined in (3). By introducing Equation (4), the regulation problem becomes a stabilization problem. The augmented system is therefore:

$$\begin{bmatrix} \dot{x} \\ \dot{x}_{int} \end{bmatrix} = \begin{bmatrix} A & 0 \\ -C & 0 \end{bmatrix} \begin{bmatrix} x \\ x_{int} \end{bmatrix} + \begin{bmatrix} B \\ 0 \end{bmatrix} u + \begin{bmatrix} 0 \\ 1 \end{bmatrix} r. \quad (5)$$

Let $\mathbf{x}_I = [x \ x_{int}]^T$, Equation (5) can be re-written as

$$\dot{\mathbf{x}}_I = \mathbf{A}_I \mathbf{x}_I + \mathbf{B}_I u + \mathbf{C}_I r. \quad (6)$$

With the PI structure in the outer loop, the control command signal will take the following form

$$u(t) = K_P \cdot e(t) + K_I \int_0^t e(\tau) d\tau = \mathbf{K} \mathbf{x}_I + K_P r. \quad (7)$$

where $\mathbf{K} = [-K_P, K_I]$.

B. Disturbance Model with Experimentally Identified Parameter

The magnetic field contributed by the neighbouring LEMA unit, (or in this study, Unit 2) results in a magnetic interference at the primary rotor R_1 which represents an input disturbance to the LEMA system (LEMA unit 1). This magnetic interference indirectly affects the angular velocity of rotor R_1 , hence the performance of the system.

The magnetic interference results in an input disturbance to the corresponding speed response on R_1 . It is essential to

know the frequency components of this disturbance signal in order to reject the disturbance. The frequency components of this disturbance can be determined by performing Fast Fourier transform (FFT) onto the speed response on R_1 with the second LEMA unit switched on.

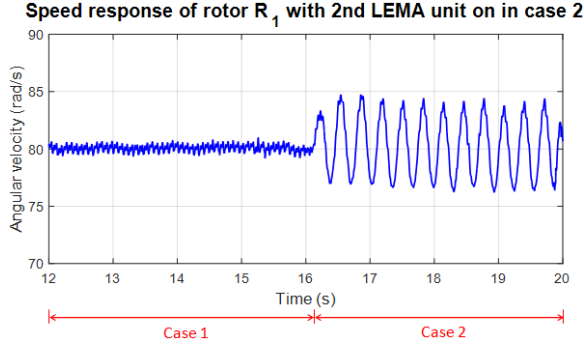


Fig. 4. Speed response for rotor, R_1 before and after LEMA unit 2 is switched on, i.e. Case 1 and Case 2 respectively. In Case 1, only LEMA unit 1 is on with reference speed of 80 rad/s and in Case 2, LEMA unit 2, which has a reference speed of 100 rad/s, is switched on.

To observe the effect of the disturbance, two sets of LEMA units are set up in experiments, where rotor R_1 is regulated (by a PI controller) to rotate at ω_{ref1} of 80rad/s (Figure 4, Case 1). The second (neighbouring) LEMA unit (Unit 2) is then activated, regulated to rotate at 100 rad/s (Figure 4, Case 2). The frequency components of the speed for rotor R_1 for Cases 1 and 2 are shown in Figures 5 and 6, respectively. The labels of Case 1 and Case 2 are consistent with that defined later in Section IV (Simulation and Experiments).

In Figure 5, the frequency components of the speed response in Case 1 can be seen at 80 rad/s alongside another component at 160 rad/s, which is due to the harmonics of the multi-DOF LEMA system that was not captured in the linearised model used in this paper. However, the effect is minimal compared to that generated by the disturbance signal due to Unit 2 (seen in Case 2, Figure 6), with the dominant frequency at 20 rad/s (the difference between the 100 rad/s disturbance signal and the 80 rad/s reference signal).

From the results above, a model of the disturbance is defined with the following form:

$$\begin{aligned} d(t) &= A_d \sin(\omega_d t + \phi), \\ \dot{d}(t) &= -A_d \omega_d^2 (\sin \omega_d t + \phi) \\ &= -A_d \omega_d^2 d(t). \end{aligned} \quad (8)$$

where only the disturbance frequency ω_d is known. In state-space representation, the disturbance is modelled as:

$$\begin{aligned} \dot{\mathbf{x}}_d &= \mathbf{A}_d \mathbf{x}_d, \\ d &= \mathbf{C}_d \mathbf{x}_d. \end{aligned} \quad (9)$$

where the disturbance state is $\mathbf{x}_d = [d(t) \quad \dot{d}(t)]^T$ and the matrices are defined as follows

$$\begin{aligned} \mathbf{A}_d &= \begin{bmatrix} 0 & 1 \\ -\omega_d^2 & 0 \end{bmatrix}, \\ \mathbf{C}_d &= [1 \quad 0]. \end{aligned} \quad (10)$$

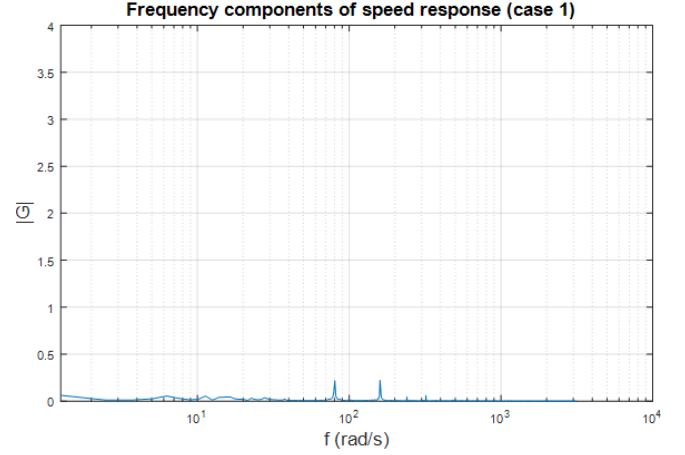


Fig. 5. Frequency component of the speed response in Case 1, showing the frequency components of reference speed on R_1 with some harmonics due to the non-linearities of the system.

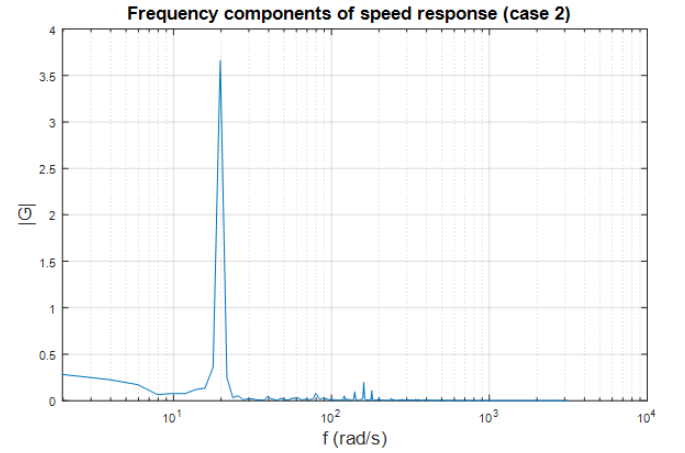


Fig. 6. Frequency component of the speed response in Case 2, showing the dominant frequency of the disturbance signal due to LEMA unit 2 which will be taken as the frequency to be rejected by IMP.

It should be noted that because the magnitude of the disturbance is identified experimentally, potentially at the system initialisation once LMA units are deployed / in place for surgery, it also implicitly captures the effect of the displacement between the stator coils and the rotor.

III. INTERNAL MODEL PRINCIPLE

IMP uses the both the disturbance (Eq. 9) and the system (Eq. 6) models to reject disturbances [20], [21]. In particular, when input disturbances are considered, the state space model of the system takes into account the disturbance, d such that

$$\dot{\mathbf{x}}_I = \mathbf{A}_I \mathbf{x}_I + \mathbf{B}_I (u + d) + \mathbf{C}_I r. \quad (11)$$

With the disturbance model (Eq. 9) augmented in Eq. 11, it has the form of

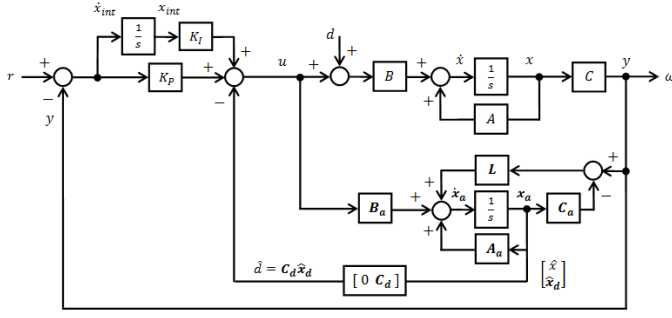


Fig. 7. Block diagram of the disturbance estimation using Internal Model Principle (IMP).

$$\begin{aligned} \dot{\mathbf{x}}_a &= \begin{bmatrix} \dot{\mathbf{x}}_I \\ \dot{\mathbf{x}}_d \end{bmatrix} = \begin{bmatrix} \mathbf{A}_I & \mathbf{B}_I \mathbf{C}_d \\ 0 & \mathbf{A}_d \end{bmatrix} \begin{bmatrix} \mathbf{x}_I \\ \mathbf{x}_d \end{bmatrix} + \begin{bmatrix} \mathbf{B}_I \\ 0 \end{bmatrix} u + \begin{bmatrix} \mathbf{C}_I \\ 0 \end{bmatrix} r. \\ &= \mathbf{A}_a \mathbf{x}_a + \mathbf{B}_a u + \mathbf{C}_a r. \\ y_a &= \begin{bmatrix} \mathbf{C}_I & 0 \end{bmatrix} \begin{bmatrix} \mathbf{x}_I \\ \mathbf{x}_d \end{bmatrix} = \mathbf{C}_a \cdot \mathbf{x}_a. \end{aligned} \quad (12)$$

Using the model above, the following observer can be designed to estimate the system and disturbance states (see Fig. 7 for block diagram):

$$\dot{\hat{\mathbf{x}}}_a = \mathbf{A}_a \hat{\mathbf{x}}_a + \mathbf{B}_a u + \mathbf{L}(y - \mathbf{C}_a \hat{\mathbf{x}}_a). \quad (13)$$

with \mathbf{L} being an observer gain such that $\mathbf{A}_a - \mathbf{L}\mathbf{C}_a$ is Hurwitz. The system was verified to be observable, and hence the gain of the observer can be assigned arbitrarily. Once the observer is designed, the control law takes the following form

$$u = \mathbf{K}\mathbf{x}_I + K_P r - \mathbf{C}_d \hat{\mathbf{x}}_d, \quad (14)$$

where \mathbf{K} and K_P comes from (7). It is noted that though all state signals are estimated, only the disturbance state is used in the control law to simplify the implementation.

By using Separation Principle [27], as long as $\mathbf{A}_I - \mathbf{B}_I \mathbf{K}$ and $\mathbf{A}_a - \mathbf{L}\mathbf{C}_a$ are both Hurwitz, the disturbance can be rejected such that $y(t)$ approaches r , which is summarized in the following theorem. The proof is provided in [27].

Theorem 1: If the matrix $\mathbf{A}_I - \mathbf{B}_I \mathbf{K}$ is Hurwitz and the $\mathbf{A}_a - \mathbf{L}\mathbf{C}_a$ is Hurwitz, then the control law (7) applied to the system (12) ensure that $\lim_{t \rightarrow \infty} y(t) = r$ and all internal state signals are bounded.

Remark 2: As the system (12) is both controllable and observable, it is possible to find \mathbf{K} and \mathbf{L} such that both the poles of $\mathbf{A}_I - \mathbf{B}_I \mathbf{K}$ and $\mathbf{A}_a - \mathbf{L}\mathbf{C}_a$ can be arbitrarily placed. The placement of the poles of the controller and the observer will depend on the performance requirement of LEMA.

Remark 3: The choice of PI parameters in the outer loop does not affect the stability of the closed loop. Moreover, the tuning of PI parameters for the LEMA system implementing FOC has been investigated in [10]. Although different choices of PI parameters will affect the system performance, it will not affect the disturbance rejection. Hence the choice of PI parameters is not the focus of this work. \circ

In general, the poles of $\mathbf{A}_a - \mathbf{L}\mathbf{C}_a$ are selected to be much faster than that of $\mathbf{A}_I - \mathbf{B}_I \mathbf{K}$ to ensure a good tracking performance.

IV. SIMULATION AND EXPERIMENTS

The disturbance of the neighbouring stator set on the primary rotor R_1 and the proposed disturbance rejection algorithm are initially validated numerically on Matlab Simulink. The resulting algorithm is also experimentally validated on an experiment platform constructed with two neighbouring LEMA units (LEMA Unit 1 and LEMA Unit 2), each unit consisting of two stator coils and a rotor. In this study, the units are placed as close as possible to one another, to create a worse case scenario of magnetic field interference.

Three cases of operation are investigated both numerically and experimentally:

- 1) Case 1: Field Oriented Control with PI controller (FOC-PI) implemented on LEMA Unit 1, while LEMA Unit 2 is not-operational. It represents the case of conventional control without disturbance, carried out as an initial benchmark.
- 2) Case 2: Field Oriented Control with PI controller (FOC-PI) implemented on LEMA Unit 1 and 2. The performance of LEMA Unit 1 is presented with the effect of having LEMA Unit 2 operating (as a source of disturbance) in its vicinity. This represents the case of conventional control with disturbance.
- 3) Case 3: Field Oriented Control with PI controller and IMP (FOC-PI-IMP), implemented on LEMA Unit 1, with LEMA Unit 2 in operation, treated as a source of disturbance. This demonstrates the effectiveness of the IMP in rejecting the present disturbance.

A. Simulation

The system model, augmented with disturbance, as well as the proposed disturbance rejection algorithm are implemented numerically on Matlab Simulink. The state space model are represented numerically based on the parameters reported in [18] reproduced in the table below, with M_i and μ_{r_i} utilised in numerically determining ψ_{R_i} in the simulation [28]:

TABLE II
MODEL PARAMETERS OF LEMA [18]

Parameters	Values
Resistance (R_S)	0.8 Ω
Inductance (L_S)	5.8 mH
Friction Coefficient (b_i)	3.9×10^{-6} Nms
Total Moment of Inertia (J_i)	6×10^{-7} kgm ²
Relative permeability of core (μ_{r_i})	5.2
Magnetization (M_i)	4.45×10^5 A/m

In the numerical simulation, LEMA Unit 1 is set to operate at 3 different reference angular velocities of 40, 60 and 80 rad/s. LEMA unit 2, which in this study serves to provide disturbance to Unit 1, is set to operate with a sinusoidal angular velocities of 100 rad/s. The disturbance frequency ω_d is identified using frequency analysis to form the disturbance model (Eq. 9) which is augmented with the IMP model (Eq.

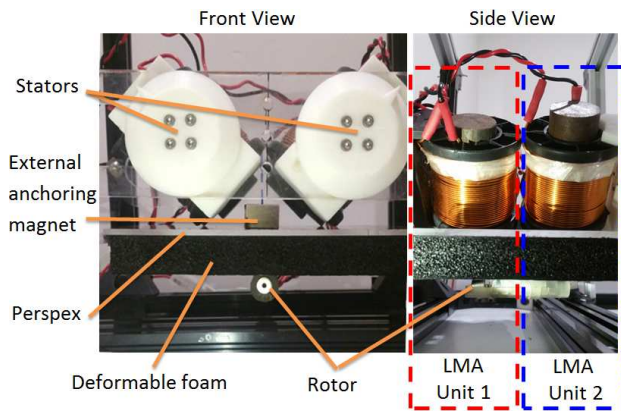


Fig. 8. The labeling of LMA Units 1 and 2 is consistent to Figure 1 to allow context. The experimental setup consist of 2 LMA units, each unit implemented using 2 electromagnetic stators (external) and one rotor (internal). The external and internal components are separated by a deformable foam representing the abdominal wall, supported by a 3mm thick perspex.

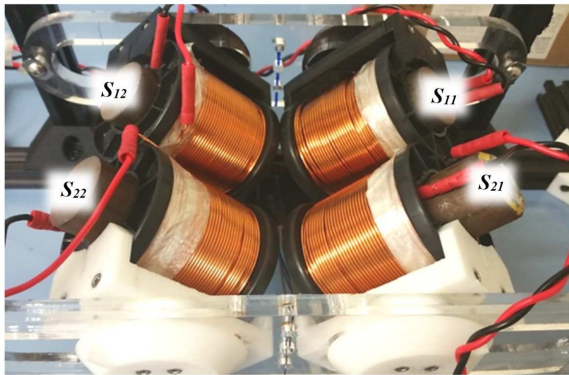


Fig. 9. A zoomed-out view of the experimental setup in Figure 8. The black deformable foam had been removed to allow easier viewing.

11). This is then utilized for obtaining the gains to the observer to estimate the disturbance to the system (Eq. 13).

The three cases (Case 1, 2, and 3) as presented in Section IV are simulated. The result is presented in Section V.

B. Experimental Setup and Procedures

Similarly, in the experimental setup, two sets of stator pairs are employed to represent a multi-DOF LEMA system, as described in the schematics shown in Fig 2. The stator coils are of 250 turns of 1.32mm copper windings. The stator coils have an outer diameter of approximately 65mm, and when placed at the closest distance together to simulate the worse case scenario for the IMP implementation, the centre of two coils would give an approximate distance of 65mm. A cylindrical Neodymium N42 permanent magnet (with dimensions 9.5 mm in diameter and length) is used as the primary rotor, R_1 and is positioned at 30mm right below stator set 1. This distance between the stators and rotor R_1 is selected to simulate the average thickness of abdominal wall tissue in an average built patient. A physical barrier in the form of a sheet of deformable foam supported by a (3mm) sheet of perspex separates the stator coils and the rotor, representing the abdominal wall (see Figure 8). In terms of the magnetic properties, the

relative permeability of the perspex piece and the sheet of foam (selected for the experimental rig) as well as the actual abdominal wall tissue are all close to that of air, thus none of them have any significant impact to the magnetic based LMA system. The thin piece of perspex is used to support the deformable foam, where in a real surgical simulation, the abdominal wall will be able to hold its shape due to insufflation. Furthermore, the stator coils in a surgical setting is also expected to be supported by a platform mounted to an external post or frame, potentially through a rigid by movable arm, thus the weight of the external unit is not resting on the abdominal wall.

External and internal permanent magnets were used to anchor the internal unit to the abdominal wall. NI myRio system is used as an interface with two Sabertooth 2×12 motor drivers for dual channel supplies to the stator units. The experiment is run with a sampling period of 1000Hz. The experimental setup is shown in Figures 8 and 9.

The same reference angular velocities of 40, 60 and 80 rad/s as in the numerical simulation are implemented experimentally over Case 1, 2 and 3. The same observer gains as those used in the respective setting in the numerical simulation also apply to the experimental operation.

V. RESULTS AND DISCUSSIONS

The results of the numerical and experimental studies are shown in Figures 10 and 11, respectively. Three sets of rotor velocities are shown: 40, 60 and 80 rad/s, on Figures 10 and 11, labelled (a), (b) and (c), respectively. Case 1, 2, and 3 for each velocity setting are marked over the x-axis.

From Figure 10, the numerical results show that for the different range of rotor velocities, FOC-PI (Case 1) performs well in the absence of disturbance, but not capable of suppressing the disturbance from LEMA Unit 2 (Case 2). Note that Figure 10 (a), (b) and (c) demonstrate different ω_d in the disturbance, where $\omega_d = 60, 40$ and 20 rad/s, respectively. Case 3 in Figure 10 (a), (b), (c) demonstrates the efficacy of the proposed FOC-PI-IMP controller in rejecting disturbance in the numerical setting.

Figure 11 demonstrates a very comparable result to that shown by the numerical study. More noise can be observed overall, as expected in a physical implementation. However, the trends remain the same. Case 1 showed an effective FOC-PI for the case of no-disturbance. Case 2 demonstrates the effect of the disturbance on the conventional FOC-PI controller when LEMA unit 2 is activated. Case 3 validates the effectiveness of FOC-PI-IMP in rejecting the disturbance produced by the actuation of Unit 2.

To provide a comparison on the frequency components of the rotor speed response in Case 3 with those in Case 1 and Case 2 to demonstrate the efficacy of the IMP controller, frequency analysis is then performed on the speed response of R_1 with the reference speed of 80 rad/s (see Figs. 5 and 6). As shown in Figure 12, the dominant frequency of the disturbance due to LEMA unit 2 has been eliminated. This demonstrates that the implementation of IMP has successfully rejected the disturbance onto rotor R_1 .

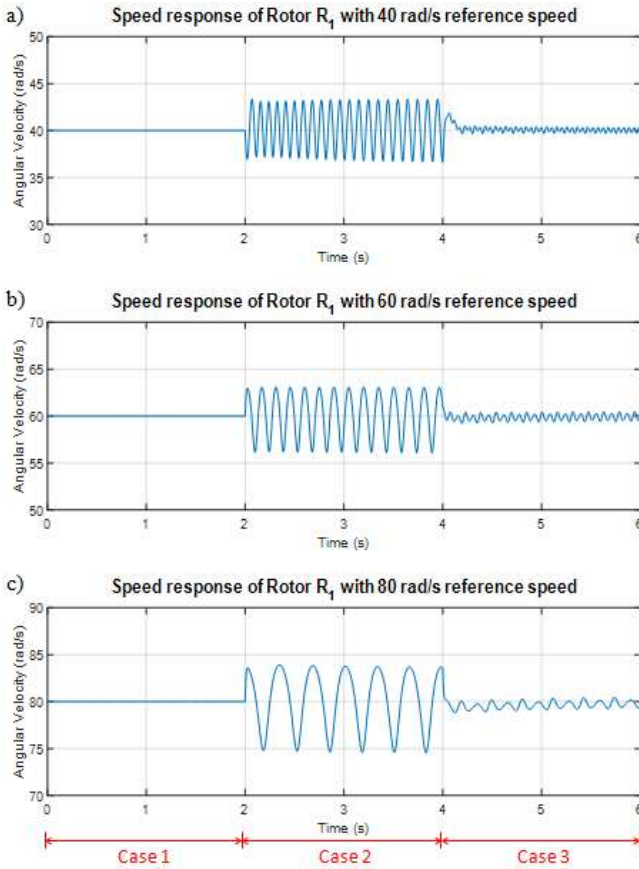


Fig. 10. Simulation results for various reference speeds, a) 40 rad/s, b) 60 rad/s, and c) 80 rad/s, with three cases: Case 1 - LEMA unit 1 implementing FOC-PI is switched on while LEMA unit 2 is non-operating, Case 2 - FOC-PI implemented on both LEMA units 1 and 2, with LEMA unit 2 generating disturbance onto rotor R_1 at a reference speed of 100 rad/s, and Case 3 - IMP is executed, demonstrating effective rejection of the disturbance from Unit 2.

Each case of the experiment was performed five times to demonstrate performance repeatability and to obtain stochastic information. Table III summarises the performance of the FOC-PI-IMP strategy for all five sets of the experimental data. The resulting performance was shown to produce an error of no more than 1 rad/s accounting for 91% of disturbance rejection in the cases across all the experiments. This also verifies that the observer designed estimates the disturbance reasonably well based on the model of the system and the partially known disturbance.

In this study, only cases where the rotors are aligned with the corresponding stator sets are considered as the effect of rotor misalignment with respect to the stator set has been thoroughly studied in [10]. It was found that the tolerance for the displacement errors due to the misalignment is sufficiently large such that the system is insensitive to the misalignment as long as it is within a distance bounded by the radius of the stator coils. The radius of the stator coils used in this study is 32.5mm, thus providing a large margin for the misalignment. In practice, the misalignment of the rotors have been found to be bounded within ± 20 mm. The use of multiple (at least 2) magnetic anchoring points also allows the internal unit to be well positioned relative to the corresponding external unit.

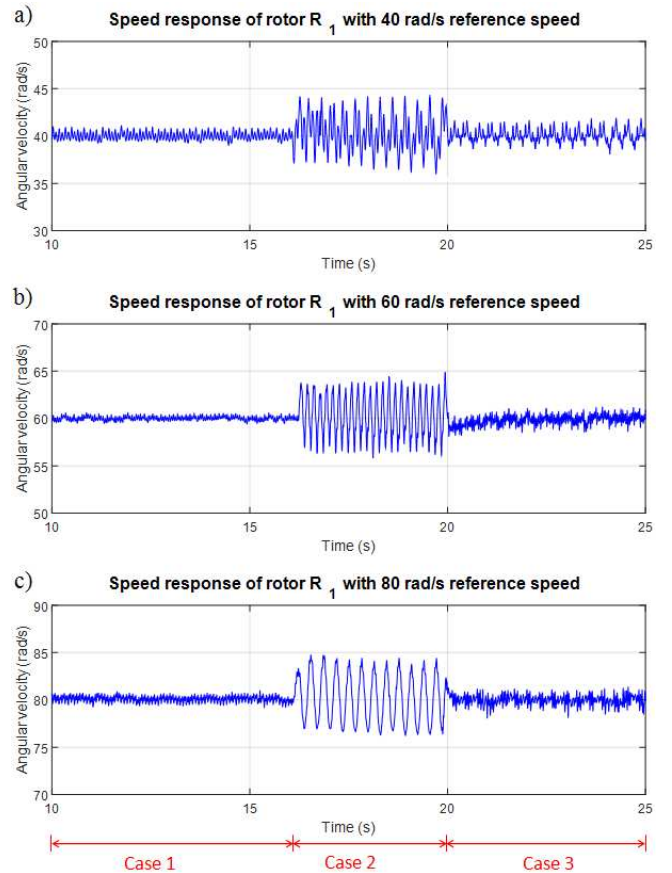


Fig. 11. Experimental results for various reference speeds, a) 40 rad/s, b) 60 rad/s, and c) 80 rad/s, with three cases: Case 1 - LEMA unit 1 implementing FOC-PI is switched on while LEMA unit 2 is non-operating, Case 2 - FOC-PI implemented on both LEMA units 1 and 2, with LEMA unit 2 generating disturbance onto rotor R_1 at a reference speed of 100 rad/s, and Case 3 - IMP is executed, demonstrating effective rejection of the disturbance from Unit 2.

VI. CONCLUSION

The Internal Model Principle (IMP) was utilised in this study to reject the systematic disturbance caused by the stray

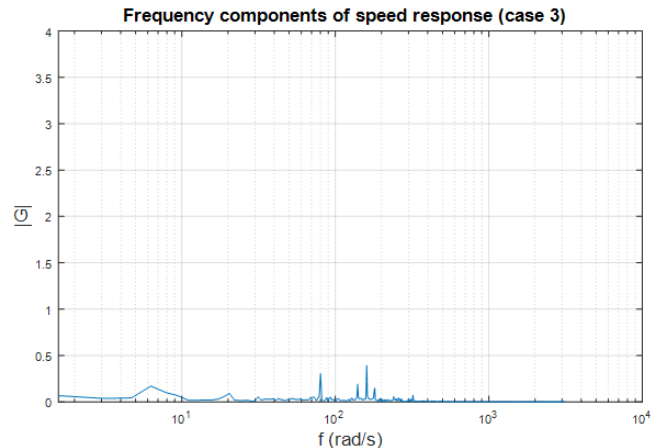


Fig. 12. Frequency component of the speed response in Case 3 (where IMP is implemented in the presence of disturbance), showing the absence of the dominant frequency of the disturbance present in Case 2. Reference R_1 speed is 80 rad/s, while speed of R_2 (serving as the disturbance) was 100 rad/s.

TABLE III

PERFORMANCE EVALUATION OF THE IMP CONTROLLER ON THE TWO-DOF LEMA EXPERIMENTAL SETUP (FROM 5 SETS OF EXPERIMENTAL DATA)

Reference speed w_{ref} (rad/s)	Case 1	Case 2	Case 3	Performance
	FOC-PI (LEMA unit 1) Steady-state amplitude, e_1 (rad/s)	FOC-PI (LEMA units 1 & 2) e_2 (rad/s)	FOC-PI-IMP (LEMA units 1 & 2) e_3 (rad/s)	Improvement (ave%) $\frac{e_2 - e_3}{e_2 - e_1} \times 100\%$
40	0.6 ± 0.2	3.9 ± 0.5	0.9 ± 0.4	90.91
60	0.4 ± 0.1	4.1 ± 0.3	0.7 ± 0.2	91.89
80	0.5 ± 0.2	4.2 ± 0.3	0.8 ± 0.3	91.89

magnetic linkage actuating a neighbouring LEMA unit. With the partial information of the disturbance, i.e. the disturbance frequency, a disturbance model can be formed to augment with the system model for IMP implementation on the conventional controller. With the availability of these models, appropriate controller and observer were designed to reject disturbances and to track the reference velocity intended for the rotor.

The strategy was demonstrated to be effective with successful disturbance suppression. The outcome can be extended to multiple (more than 2) DOF LMA systems without loss of generality. Future work will include the dynamics of the manipulator into the control consideration.

REFERENCES

- [1] F. Leong, N. Garbin, C. DiNatali, A. Mohammadi, D. Thiruchelvam, D. Oetomo, and P. Valdastrì, "Magnetic Surgical Instruments for Robotic Abdominal Surgery", *IEEE Revs Biomed Eng*, vol. 9, pp. 66–78, 2016.
- [2] S. Park, R. A. Bergs, R. Eberhart, L. Baker, R. Fernandez, and J. A. Cadeddu, "Trocar-less instrumentation for laparoscopy: magnetic positioning of intra-abdominal camera and retractor", *Ann Surg*, vol. 245, no. 3, pp. 379, 2007.
- [3] J. Cadeddu, R. Fernandez, M. Desai, R. Bergs, C. Tracy, S.-J. Tang, P. Rao, M. Desai, and D. Scott, "Novel magnetically guided intra-abdominal camera to facilitate laparoendoscopic single-site surgery: initial human experience", *Surg Endosc*, vol. 23, no. 8, pp. 1894–1899, 2009.
- [4] M. P. Kummer, J. J. Abbott, B. E. Kratochvil, R. Borer, A. Sengul, and B. J. Nelson, "Octomag: An electromagnetic system for 5-DOF wireless micromanipulation", *IEEE Trans. Robotics*, vol. 26, no. 6, pp. 1006–1017, 2010.
- [5] F. Carpi, S. Galbiati, and A. Carpi, "Controlled navigation of endoscopic capsules: concept and preliminary experimental investigations", *IEEE Trans Biomed Eng*, vol. 54, no. 11, pp. 2028–2036, 2007.
- [6] J. J. Abbott, O. Ergeneman, M. P. Kummer, A. M. Hirt, and B. J. Nelson, "Modeling magnetic torque and force for controlled manipulation of soft-magnetic bodies", *IEEE Trans. Robotics*, vol. 23, no. 6, pp. 1247–1252, 2007.
- [7] A. W. Mahoney, and J. J. Abbott, "Generating rotating magnetic fields with a single permanent magnet for propulsion of untethered magnetic devices in a lumen", *IEEE Trans. on Robotics*, vol. 30, no. 2, pp. 411–420, 2014.
- [8] G. Tortora, M. Salerno, T. Ranzani, S. Tognarelli, P. Dario, and A. Menciassi, "A modular magnetic platform for natural orifice transluminal endoscopic surgery", in *Procs. IEEE Eng Med Biol Soc*, pp. 6265–6268, 2013.
- [9] D. Oleynikov, "Robotic surgery", *Surg Clin North Am*, vol. 88, no. 5, pp. 1121–1130, 2008.
- [10] A. Mohammadi, D. Samsonas, F. Leong, Y. Tan, D. Thiruchelvam, P. Valdastrì, and D. Oetomo, "Modelling and Control of Local Electromagnetic Actuation for Robotic-Assisted Surgical Devices", *IEEE/ASME Trans Mechatronics*, vol. 22, no. 6, pp. 2449–2460, 2017.
- [11] M. Cadeddu, M. Boyd, and P. Swain, "Retraction force measurement during transgastric and transvaginal notes, *Gastrointest Endosc*, vol. 6, no. 5, pp. AB119, 2008.
- [12] F. Leong, W.H. Huang and C.K. Chui, "Modeling and analysis of coagulated liver tissue and its interaction with a scalpel blade", *Med Biol Eng Comput*, vol. 51, no. 6, pp. 687–695, 2013.
- [13] A.M. Okamura, C. Simone and M.D. O'Leary, "Force modeling for needle insertion into soft tissue", *IEEE Trans Biomed Eng*, vol. 51, no. 10, pp. 1707–1716, 2004.
- [14] T.B. Frick, D.D. Marucci, J.A. Cartmill, C.J. Martin and W.R. Walsh, "Resistance forces acting on suture needles", *J Biomechanics*, vol. 34, no. 10, pp. 1335–1340, 2001.
- [15] T. Horeman, M.D. Blikkendaal, D. Feng, A. van Dijke, F. Jansen, J. Dankelman and J.J. van den Dobbelsteen, "Visual force feedback improves knot-tying security", *J Surg Educ*, vol. 71, no. 1, pp. 133–141, 2014.
- [16] C. Di Natali, J. Buzzi, N. Garbin, M. Beccani and P. Valdastrì, "Closed-loop control of local magnetic actuation for robotic surgical instruments", *IEEE Trans. Robotics*, vol. 31, no. 1, pp. 143–156, 2015.
- [17] N. Garbin, C. Di Natali, J. Buzzi, E. De Momi, and P. Valdastrì, "Laparoscopic tissue retractor based on local magnetic actuation", *J Med Dev*, vol. 9, no. 1, pp. 011005, 2015.
- [18] F. Leong, A. Mohammadi, Y. Tan, D. Thiruchelvam, P. Valdastrì, and D. Oetomo, "Magnetic Interactions of Neighbouring Stator Sets in Multi DOF Local Electromagnetic Actuation for Robotic Abdominal Surgery", in *Procs. IEEE/RSJ Int. Conf. Intell. Robots Syst.*, 2017.
- [19] Pethig, R. and Kell, D.B., "The passive electrical properties of biological systems: their significance in physiology, biophysics and biotechnology", *Phys. Med. Biol*, vol. 32, no. 8, pp. 933, 1987.
- [20] P. Hippe, and J. Deutscher, "Disturbance Rejection Using the Internal Model Principle. Design of Observer-based Compensators: From the Time to the Frequency Domain", Springer Science & Business Media, pp. 131–166, 2009.
- [21] I. D. Landau, A. Constantinescu, and D. Rey, "Adaptive narrow band disturbance rejection applied to an active suspensionan internal model principle approach", *Automatica*, vol. 41, no. 4, pp. 563–574, 2005.
- [22] A. Mohammadi, D. Samsonas, C. Di Natali, P. Valdastrì, Y. Tan, and D. Oetomo, "Speed control of non-collocated stator-rotor synchronous motor with application in robotic surgery", in *Procs. Asian Control Conf.*, pp. 1–6, 2015.
- [23] P. C. Sen, "Electric motor drives and control-past, present, and future", *IEEE Trans. Ind. Electron*, vol. 37, no. 6, pp. 562–575, 1990.
- [24] Z. Wang, J. Chen, M. Cheng and K. T. Chau, "Field-oriented control and direct torque control for paralleled VSIs fed PMSM drives with variable switching frequencies", *IEEE Trans. Power Electron*, vol. 31, no. 3, pp. 2417–2428, 2016.
- [25] T. S. Low, T. H. Lee, K. J. Tseng, and K. S. Lock, "Servo performance of a BLDC drive with instantaneous torque control", *IEEE Trans. Ind. Appl.*, vol. 28, no. 2, pp. 455–462, 1992.
- [26] H. K. Khalil, "Nonlinear Systems", Prentice-Hall, New Jersey, 2nd Edition, Chapter 9, pp.351–388, 1996.
- [27] G. C. Goodwin, S. F. Graebe, and M. E. Salgado, "Control System Design", Chapter 10, pp. 263–286, 2000.
- [28] F. Leong, A. Mohammadi, Y. Tan, P. Valdastrì and D. Oetomo, "Experimentally Validated Modelling of Electromechanical Dynamics on Local Magnetic Actuation System for Abdominal Surgery", in *Procs. Australasian Conf Robot Autom*, 2016.
- [29] G. Hang, M. Bain, J. Y. Chang, S. Fang, F. Leong, A. Mohammadi, P. Valdastrì and D. Oetomo, "Local Magnetic Actuation Based Laparoscopic Camera for Minimally Invasive Surgery", in *Procs. Australasian Conf Robot Autom*, 2015.